

Binding of ^{15}N -Labeled Isoniazid to KatG and KatG(S315T): Use of Two-Spin [zz]-Order Relaxation Rate for ^{15}N –Fe Distance Determination

Smilja Todorović,^{†,‡,§} Nenad Juranić,[†] Slobodan Macura,[†] and Frank Rusnak^{*,†,‡}

Contribution from the Department of Biochemistry and Molecular Biology, Section of Hematology Research, Mayo Clinic and Foundation, Rochester, Minnesota 55905, and Faculty of Physical Chemistry, University of Belgrade, Belgrade, Yugoslavia

Received June 4, 1999. Revised Manuscript Received September 7, 1999

Abstract: Isoniazid has been used to treat tuberculosis for over 40 years, but its mechanism of action is not yet fully understood. It is known that a catalase/peroxidase KatG is required for isoniazid activation. A point mutation in KatG, KatG(S315T), is found in >50% of isoniazid-resistant strains. In this study we have measured the distance between the ^{15}N labeled amide nitrogen of isoniazid and the Fe ion in the active site of KatG and KatG(S315T). The distances are found to be equal within experimental error, 3.8 ± 0.8 and 4.4 ± 0.9 Å, respectively. A new method of measuring longitudinal relaxation rates of insensitive nuclei in paramagnetic systems via zz-order is proposed. The longitudinal relaxation rate of the ^{15}N nucleus was obtained from the independently measured longitudinal proton relaxation rate and the longitudinal zz-order relaxation rate of scalar coupled N and H atoms. To eliminate cross-correlations of different relaxation sources, a remote proton was used to create zz-order and detect the ^{15}N nucleus. The obtained ^{15}N –Fe distances are significantly shorter than previously reported ^1H –Fe distances (Wengenack, N. L.; Todorovic, S.; Yu, L.; Rusnak, F. *Biochemistry* **1998**, *37*, 15825), indicating that the isoniazid molecule approaches the heme Fe ion via the hydrazine nitrogen atoms. The proposed method for two-spin order relaxation measurements is quite general and can be used to probe the distance between insensitive nuclei and a paramagnetic center in various protein–substrate complexes.

Introduction

Mycobacterium tuberculosis KatG is a catalase-peroxidase consisting of two 82 kDa subunits, each containing an Fe–protoporphyrin IX cofactor.^{1,2} Other enzymatic activities have been attributed to KatG, namely a Mn(II) dependent peroxidase activity analogous to the manganese peroxidase of *Phanerochaete chrysosporium*,^{2–4} as well as P₄₅₀-like monooxygenase^{2,5} and peroxynitritase activities.⁶ Moreover, it has been hypothesized that KatG is responsible for converting isoniazid (INH, isonicotinic acid hydrazide), the most widely used antituberculosis drug for over 40 years, into an activated form.^{2,7} The mechanism of this in vivo activation is still unknown but it is clear that a functional form of KatG is necessary.^{2,8} Recent work suggests that activated INH acts as an inhibitor of enzymes

involved in mycolic acid biosynthesis, thereby disrupting the permeability barrier of the mycobacteria cell wall.^{2,9}

A point mutation in KatG in which serine at amino acid residue 315 is replaced by threonine, KatG(S315T), is the most common mutation found in INH-resistant strains of KatG.^{9–11} A three-dimensional structure of KatG is not available, but it is believed that KatG shares a similar active-site architecture with cytochrome *c* peroxidase since they belong to the same class of the catalase-peroxidase superfamily.¹² By this analogy, amino acid residue 315 has been modeled near the active site of KatG;¹³ a point mutation at this residue could very likely alter the enzymatic activity of KatG. Interestingly, however, it appears that KatG(S315T) is a competent catalase/peroxidase with only a 2-fold difference in catalytic efficiency of peroxidase activity compared to wild-type enzyme.¹⁴ Nevertheless, in the presence of oxygen, INH is oxidized to isonicotinic acid by both KatG and KatG(S315T), but the rate of oxidation of INH by KatG(S315T) is reduced compared to the wild-type enzyme.¹⁴

* To whom correspondence should be addressed at Mayo Clinic and Foundation.

[†] Department of Biochemistry and Molecular Biology.

[‡] Section of Hematology Research.

[§] University of Belgrade.

(1) Johnsson, K.; Froland, W. A.; Schultz, P. G. *J. Biol. Chem.* **1997**, *272*, 2834.

(2) Wengenack, N. L.; Todorovic, S.; Yu, L.; Rusnak, F. *Biochemistry* **1998**, *37*, 15825.

(3) Zabinski, R. F.; Blanchard, J. S. *J. Am. Chem. Soc.* **1997**, *119*, 2331.

(4) Magliozzo, R. S.; Marcinkeviciene, J. A. *J. Biol. Chem.* **1997**, *272*, 8867.

(5) Magliozzo, R. S.; Marcinkeviciene, J. A. *J. Am. Chem. Soc.* **1996**, *118*, 11303.

(6) Wengenack, N. L.; Jensen, M. P.; Rusnak, F.; Stern, M. K. *Biochem. Biophys. Res. Commun.* **1999**, *256*, 485.

(7) Riley, L. W. In *Tuberculosis*; Rom, W. N., Garay, S., Eds.; Little, Brown & Co.: Boston, 1996; pp 763–771.

(8) Johnsson, K.; Schultz, P. G. *J. Am. Chem. Soc.* **1994**, *116*, 7425.

(9) Connell, N. D.; Nikaido, H. In *Tuberculosis: Pathogenesis, Protection and Control*; Bloom, B. R., Ed.; ASM Press: Washington, DC, 1994; pp 333–352.

(10) Musser, J. M.; Kapur, V.; Williams, D. L.; Kreiswirth, B. N.; van Soolingen, D.; van Embden, J. D. A. *J. Infect. Dis.* **1996**, *137*, 196.

(11) Victor, T. C.; Pretorius, G. S.; Felix, J. V.; Jordaan, A. M.; van Helden, P. D.; Eisenach, K. D. *Antimicrob. Agents Chemother.* **1996**, *40*, 1572.

(12) Fintzel, B. C.; Poulos, T. L.; Kraut, J. *J. Biol. Chem.* **1984**, *259*, 13027.

(13) Heym, B.; Alzari, P. M.; Honore, N.; Cole, S. T. *Mol. Microbiol.* **1995**, *15*, 235.

(14) Wengenack, N. L.; Uhl, J. R.; Amand, A. L. S.; Tomlinson, A. J.; Benson, L. M.; Naylor, S.; Kline, B. C.; Cockerill, F. R., III; Rusnak, F. *J. Infect. Dis.* **1997**, *176*, 722.

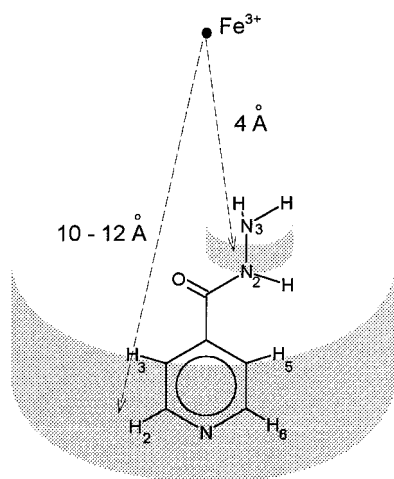


Figure 1. Structure of INH depicting relative positions of ring protons and the nitrogen atom (N_2), used for zz -order relaxation measurements, with respect to the paramagnetic center of KatG. The two shaded areas are meant to represent the uncertainty in ^1H -Fe and ^{15}N -Fe distances obtained by NMR relaxation measurements. These uncertainties are larger than the experimental error and originate from two possible sources. First, because of a possible rotation of the INH ring which will weaken the dipole-dipole interaction, the measured ^1H -Fe distance is obtained between the Fe center and a point anywhere beyond the $\text{H}_{3,5}$ (symbolized by the lower shaded area). This results in measured distances that are greater than or equal to the actual distance of the INH-KatG complex. Second, due to dipole-dipole and/or scalar interaction between N_2 and N_3 , the effective distance from N_2 to Fe is measured from any point between the two nitrogen atoms and the Fe center (upper shaded area).

In the resting state of KatG the Fe ion exists in the ferric oxidation state and is therefore highly paramagnetic.^{2,15,16} Due to dipolar interactions with unpaired electron spins, relaxation rates of substrate atoms that bind in the proximity of the paramagnetic center are affected and can be used to calculate the distance of substrate nuclei to the paramagnetic center by use of the Solomon-Bloembergen equation.¹⁷⁻¹⁹ Typical Fe- ^1H distances for aromatic substrate molecules reported for heme proteins fall in the range from 3.4 to 12 Å.²⁰⁻²⁵ There are very few reports of the application of this method for nuclei other than a proton.²⁶

In the present study, we report the distance of the amide nitrogen atom of INH (N_2 , Figure 1) to the Fe ion of KatG and KatG(S315T). Determination of ^{15}N -Fe distances may provide clues to the molecular basis for INH resistance of KatG(S315T). In principle, longitudinal relaxation rates can be measured by a standard inversion-recovery NMR experiment and ^{15}N -Fe distances can be determined by use of the Solomon-Bloembergen equation. This method, however, has inherent limitations due to the low sensitivity of direct ^{15}N NMR spectroscopy

($\sim 10^{-4}$ compared to ^1H NMR) that cannot be circumvented even with isotope enrichment. Most often indirect detection significantly improves sensitivity, but in the present case there are two problems. For isotope enriched [$^{15}\text{N}_2, ^{15}\text{N}_3$]-INH, the hydrazine protons are in fast exchange with water protons thereby impeding indirect detection of the ^{15}N signal through the directly attached proton. Even if these protons were observable, dipolar interactions with the nitrogen spin and with nitrogen chemical shift anisotropy would induce serious errors in measured ^{15}N relaxation rates due to cross-correlation effects.²⁷ The alternative is to use [$^{15}\text{N}_2, ^{15}\text{N}_3$]-INH dissolved in D_2O to eliminate exchangeable protons and to detect ^{15}N via remotely coupled ring protons ($\text{H}_{3,5}$, Figure 1). However, coupling constants of remote nuclei are an order of magnitude smaller than for directly bonded nuclei, and consequently, much longer times for coupling constant evolution ($\propto J^{-1}$) are required. As a result, the majority of the nitrogen signal is lost during this period due to the short T_2 of nitrogen. Thus, in paramagnetic complexes, fast transverse relaxation of ^{15}N does not allow the indirect detection of ^{15}N relaxation via remote protons.

In this report we introduce a novel method that facilitates indirect detection of the amide nitrogen ($^{15}\text{N}_2$, Figure 1) using scalar coupling to a remote nuclear spin of INH ring protons ($\text{H}_{3,5}$, Figure 1). Although this spin system precludes standard measurements of ^{15}N relaxation measurements, it still allows the detection of proton-nitrogen two-spin order.^{27,28} We show by a simple analysis that the longitudinal ^{15}N relaxation rate in a paramagnetic complex can be extracted from the longitudinal relaxation rates of protons and zz -order of remotely coupled spins. This allowed us to determine the ^{15}N -Fe distances of substrate-protein complexes for KatG and KatG(S315T) by use of the Solomon-Bloembergen equation.

Theoretical Background

In a three-spin system, with two spins (^{15}N and ^1H) relaxing through dipolar coupling with a rapidly relaxing electron (S), the evolution of the two-spin order is given by:²⁷

$$-\frac{d}{dt}\langle 2H_z N_z(t) \rangle = K_H \xi_{\text{HN}} \Delta \langle H_z(t) \rangle + K_N \xi_{\text{HN}} \Delta \langle N_z(t) \rangle + R_{\text{1HN}} \langle 2H_z N_z(t) \rangle \quad (1)$$

Here, $\Delta \langle H_z \rangle$ and $\Delta \langle N_z \rangle$ are deviations from equilibrium of ^1H and ^{15}N longitudinal magnetizations, respectively, $\langle 2H_z N_z \rangle$ represents the zz -order, and R_{1HN} is the zz -order relaxation rate constant. The coefficient ξ_{HN} gauges the strength of ^1H - ^{15}N dipolar interaction, $\xi_{\text{HN}} \propto 1/(r_{\text{H-N}})^3$, where $r_{\text{H-N}}$ is the interspin distance. The coefficients K take into account cross-correlation between electron-nucleus and nucleus-nucleus dipolar interaction. Cross-correlation effects introduce nonexponential decay of zz -order, eq 1, and in the present case are undesirable. If the nuclear spins are remote, the internuclear dipolar interaction becomes negligible, $\xi_{\text{HN}} \approx 0$, the first two terms in eq 1 can be neglected, and zz -order relaxes monoexponentially. The relaxation rate constant of zz -order, R_{1HN} , can be written as:²⁷

$$R_{\text{1HN}} = \xi_{\text{HS}}^2 \left[\frac{7}{3} j(\omega_s) + j(\omega_{\text{H}}) \right] + \xi_{\text{NS}}^2 \left[\frac{7}{3} j(\omega_s) + j(\omega_{\text{N}}) \right] \quad (2a)$$

or more generally, as the sum of longitudinal paramagnetic

- (15) Bertini, I.; Turano, P.; Vila, A. *J. Chem. Rev.* **1993**, *93*, 2833.
 (16) Yamamoto, Y. *Ann. Rep. NMR Spectrosc.* **1998**, *36*, 1.
 (17) Solomon, I. *Phys. Rev.* **1955**, *99*, 559.
 (18) Bloembergen, N. *J. Chem. Phys.* **1957**, *27*, 572.
 (19) Bloembergen, N.; Morgan, L. O. *J. Chem. Phys.* **1961**, *34*, 842.
 (20) Modi, S.; Primrose, W. U.; Boyle, J. M. B.; Gibson, C. F.; Lian, L.; Roberts, G. C. K. *Biochemistry*, **1995**, *34*, 8982.
 (21) Sakurada, J.; Takahashi, S.; Hosoya T. *J. Biol. Chem.* **1986**, *261*, 9657.
 (22) Koerts, J.; Rietjens, I. M. C. M.; Boersma, M. G.; Vervoort J. *FEBS Lett* **1995**, *368*, 279.
 (23) Novak, R. F.; Vastis, K. P. *Mol. Pharm.* **1982**, *21*, 701.
 (24) Modi S.; Gilham, D. E.; Sutcliffe, M. J.; Lian, L.-Y.; Primrose, W. U.; Wolf, C. R.; Roberts, G. C. K. *Biochemistry* **1997**, *36*, 4461.
 (25) Veitch, N. C. *Biochem. Soc. Trans.* **1995**, *23*, 232.
 (26) Wilkens, S. J.; Xia, B.; Volkman, B. F.; Weinhold, F.; Markley, J. L.; Westler, W. M. *J. Phys. Chem. B* **1998**, *102*, 8300.

- (27) Werbelow, L. G.; Thevand, A. *J. Magn. Reson.* **1993**, *A 101*, 317.
 (28) Peng, J. W.; Wagner, G. In *Nuclear Magnetic Resonance Probes of Molecular Dynamics*; Tyco, R., Ed.; Kluwer Academic Publishers: Boston, 1994; pp 373-454.

relaxation rates for respective nuclei:

$$R_{\text{IHN}} = R_{\text{IH}} + R_{\text{IN}} \quad (2b)$$

Coefficients ξ_{iS} gauge respective electron–nuclear dipole–dipole interactions and for a paramagnetic system with electron spin S and nucleus with gyromagnetic ratio γ_i ($i = \text{H, N}$), $\xi_{iS} = [6S(S+1)/15]^{1/2}(\mu_0/4\pi)[\gamma_i\gamma_S\hbar/r_{i-S}^3]$, where \hbar is Planck's constant, μ_0 is the magnetic permeability in a vacuum, and r_{i-S} is the distance between the paramagnetic center with electron spin S and nucleus i .

Thus, in the three spin ^1H – ^{15}N –Fe system of the INH–KatG complex, the longitudinal relaxation rate of the insensitive ^{15}N nucleus can be obtained from the longitudinal relaxation rates of two-spin order and the remotely coupled proton of a bound substrate:

$$R_{\text{IN}} = R_{\text{IHN}} - R_{\text{IH}} \quad (2c)$$

However, if the substrate molecules are in fast exchange between free and bound states, the measured longitudinal relaxation rate R_{Iobs} ($1/T_{\text{Iobs}}$) is the weighted average of relaxation rates of free and bound substrate molecules, R_{If} ($=1/T_{\text{If}}$), and R_{Ib} ($=1/T_{\text{Ib}}$), respectively:

$$R_{\text{Iobs}} = p_{\text{f}}R_{\text{If}} + p_{\text{b}}R_{\text{Ib}} \quad (3)$$

where p_{f} and p_{b} are molar fractions of free and bound ligand, respectively.

The paramagnetic contribution to the relaxation rate of a bound substrate nucleus, R_{Ib} , can be extracted for both proton, R_{IH} , and zz -order, R_{IHN} , relaxation by application of eq 3. It is related to the nucleus–Fe ion distance by the Solomon–Bloembergen equation.^{2,20–24} By taking $\tau_{\text{e}} = 5 \times 10^{-11}$ s,²¹ assuming the high-spin ferric state of the protein ($S = 5/2$), and noting that $\omega_{\text{H}}^2\tau_{\text{c}}^2 \ll 1$, $\omega_{\text{S}}^2\tau_{\text{c}}^2 \gg 1$,²⁹ the Solomon–Bloembergen equation gives the distances of the Fe ion to (a) ^1H :

$$r_{\text{Fe-H}}(m) = (1.8739 \times 10^{-9})[T_{\text{IH}}(s)]^{1/6} \quad (4a)$$

and (b) ^{15}N :

$$r_{\text{Fe-N}}(m) = (0.8738 \times 10^{-9})[T_{\text{IN}}(s)]^{1/6} \quad (4b)$$

Longitudinal relaxation times, T_{IH} and T_{IN} , correspond to relaxation times of bound substrate nuclei, proton, and nitrogen, respectively.

Materials and Methods

Chemicals. Hydrazine sulfate ($^{15}\text{N}_2$, 98%) and deuterium oxide (99.9%) were purchased from Cambridge Isotope Laboratories (Andover, MA). Isonicotinic acid ethylester and sodium hydroxide were purchased from Sigma Chemical Company (St. Louis, MO). Tris base, sodium phosphate monobasic, and sodium phosphate dibasic were purchased from Curtin Matheson Scientific (Houston, TX). Coomassie Plus Protein Assay Reagent was purchased from Pierce (Rockford, IL).

Protein Purification and Ligand Binding Constants. *M. tuberculosis* KatG and KatG(S315T) were overexpressed in *Escherichia coli* and purified as previously described.^{2,14} Protein concentrations were determined using Pierce Coomassie Plus Protein Assay Reagent with bovine serum albumin as the standard.³⁰

Binding constants of INH for KatG and KatG(S315T) and the determination of molar fraction of bound ligand, p_{b} , were reported previously.^{2,14}

[$^{15}\text{N}_2$, $^{15}\text{N}_3$]-INH Synthesis. The synthesis was carried out following the methods of Rohllich and Matsuki et al., reported for synthesis of deuterium-labeled INH from isonicotinic acid *N*-oxide.^{31,32} In this modified version, commercially available [^{15}N]- $\text{N}_2\text{H}_4 \cdot \text{H}_2\text{SO}_4$ was the precursor in the synthesis. Two equivalents of solid sodium hydroxide, dissolved in 0.5 mL of water, were added to 0.5 g of [^{15}N] hydrazine sulfate. The slurry was centrifuged to remove the precipitated sodium sulfate. The liquid phase, containing [^{15}N]- N_2H_4 , was collected and the pH adjusted to 13 by addition of NaOH. One equivalent of isonicotinic acid ethyl ester was added to 0.5 mL of [^{15}N]- N_2H_4 . The mixture was refluxed for 30 min at the lowest possible temperature and subsequently cooled to 0 °C at which point a yellow solid precipitated. The precipitate was dissolved in a minimum volume of water and purified by HPLC chromatography using a semipreparative (250 × 10 mm) Microsorb Reverse Phase C18 Column (Rainin Instruments, Woburn, MA). A linear gradient method, using 50 mM ammonium acetate (pH 7)/acetonitrile as the mobile phase, changing from 95/5 to 20/80 ratio over 10 min, was employed. Detection of products was at 260 nm. Three major products with retention times 2.2, 3.2, and 7.24 min (1 mL/min flow) and relative ratios of 18, 76, and 6% were identified as isonicotinic acid, isonicotinic acid hydrazide, and isonicotinic acid ethylester, respectively. Fractions, containing [$^{15}\text{N}_2$, $^{15}\text{N}_3$]-INH were collected and lyophilized. Total yield of [$^{15}\text{N}_2$, $^{15}\text{N}_3$]-INH was ~0.15 g; the purity was confirmed by HPLC using an analytical RP C18 column (150 × 4.6 mm) and ^1H NMR.

NMR Spectroscopy. ^1H NMR measurements were carried out on a Bruker Avance 500 MHz spectrometer at 25 °C. Samples contained 25 mM [$^{15}\text{N}_2$, $^{15}\text{N}_3$]-INH in D_2O , while the enzyme concentration was varied from 60 to 240 μM by adding aliquots of wild-type KatG (1.2 mM in 5 mM phosphate buffer/ D_2O , pH 7.5) or KatG(S315T) (1.1 mM in 5 mM phosphate buffer/ D_2O , pH 7.5) directly to the substrate sample. All samples were degassed with argon to remove oxygen and kept anaerobic by use of a Wilmad Omni-fit NMR tube.

Proton longitudinal relaxation rates were determined using the $[180^\circ - \tau - 90^\circ(\text{FID}) - T_{\text{D}}]_n$ pulse sequence and zz -order by the sequence described by Kay et al.³³ Relaxation times were varied from 5 to 800 ms, and repetition time was set to 2 s. The coupling constant between N_2 and $\text{H}_{3,5}$ (Figure 1), J_{NH} , was found to be ~2 Hz and the J -evolution time (Δ) for zz -order was set to 85 ms. To reduce the artifacts of indirect detection, 2D spectra were collected. Phase sensitive (TPPI) spectra with 64 scans were recorded over 17 ppm in the F2 (1024 data points) and 40 ppm in the F1 (128 data points) dimensions. Data were filtered by Lorentz to Gauss transformation in F2 and squared sine-bell in F1 dimensions. A peak volume of $\delta_{\text{H}} = 7.6$ ppm/ $\delta_{\text{N}} = 131$ ppm cross-peak was measured.

Results

Two-spin order relaxation rates, $R_{\text{IHN(obs)}}$, were determined from the slope of a plot of $\ln(I/I_0)$ versus relaxation time, Figure 2, where I and I_0 are the $\delta_{\text{H}} = 7.6$ ppm/ $\delta_{\text{N}} = 131$ ppm cross-peak volumes at time t and at time zero, respectively.

Figure 2 shows that zz -order relaxation is monoexponential, as predicted by eq 1 for $\xi_{\text{HN}} \approx 0$. Moreover, it shows that the zz -order relaxation rate increases with protein concentration, indicating that INH binds near the paramagnetic center. For the highest protein concentration, zz -order relaxes so quickly that signal is practically lost after 40 ms relaxation time.

Figures 3A and 3B show the longitudinal proton relaxation (○) and the longitudinal zz -order relaxation (●) as a function of the fraction of INH bound to the protein, p_{b} , for wild-type

(31) Rohllich, M. *Arch. Pharm.* **1951**, 284, 6.

(32) Matsuki, Y.; Katakuse, Y.; Katashima, M.; Matsuura, H.; Goromaru, T. *Chem. Pharm. Bull.* **1989**, 37(6) 1637.

(33) Kay, L.; Nicholson, L. K.; Delaglio, F.; Bax, A.; Torchia, D. A. *J. Magn. Reson.* **1992**, 97, 359.

(29) Wütrich, K. In *NMR of Protein and Nucleic Acids*; J. Wiley Publishers: New York, 1986; p 27.

(30) Bradford, M. M. *Anal. Biochem.* **1976**, 72, 248.

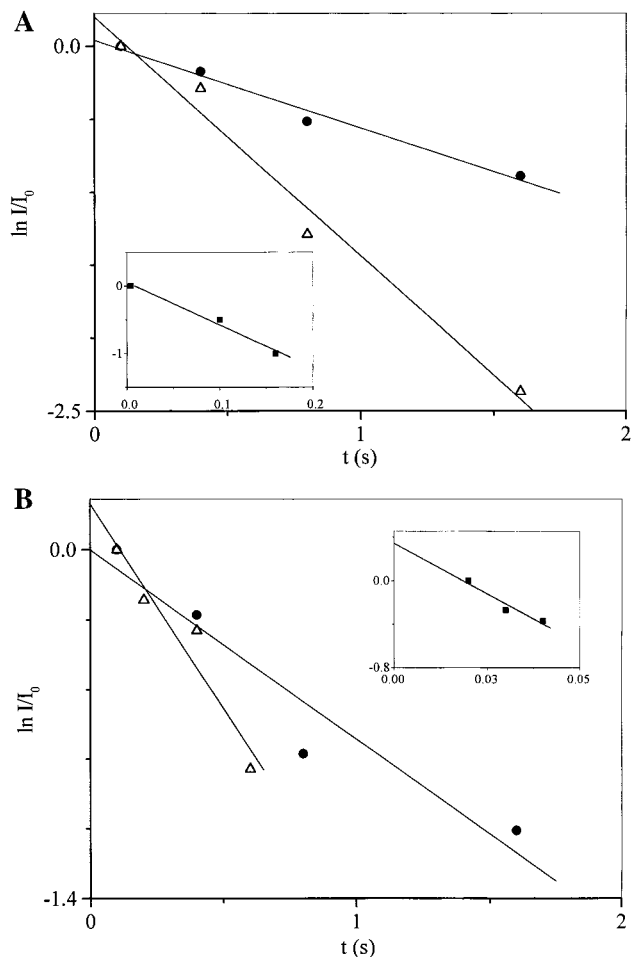


Figure 2. Determination of $R_{\text{IHN(obs)}}$, the longitudinal relaxation rate for zz -order of the $\text{N}_2\text{-H}_{3,5}$ nuclei in the presence of a varying concentration of KatG (A) and KatG(S315T) (B). Plot of $\ln(I/I_0)$, logarithm of the normalized volume of the ($\text{N}_2\text{-H}_{3,5}$) cross-peak ($\delta_{\text{H}} = 7.6 \text{ ppm}/\delta_{\text{N}} = 131 \text{ ppm}$) of 25 mM INH (Figure 1) as a function of relaxation time, t (s). The concentrations of proteins were 60 (●), 160 (Δ), and 240 μM (■) (inset) in A and 60 (●), 140 (Δ), and 210 μM (■) (inset) for KatG(S315T) in B. The slope of the plot yields $R_{\text{IHN(obs)}}$.

KatG and for KatG(S315T), respectively. Relaxation rates of ring protons, R_{IH} , and relaxation rates of zz -order, R_{IHN} , of INH bound to the protein were obtained from the slopes of data fitted to eq 3. For both enzymes, $R_{\text{IHN}} = 200 \pm 30 \text{ s}^{-1}$ whereas $R_{\text{IH}} = 45 \pm 5 \text{ s}^{-1}$ for KatG, and $R_{\text{IH}} = 130 \pm 6 \text{ s}^{-1}$ for KatG(S315T). In the absence of protein, $p_b = 0$, the relaxation rates of proton and zz -order converge. This implies that the nitrogen relaxation in the free ligand is much slower than proton relaxation, as expected. With the addition of the paramagnetic protein, zz -order decays faster than the proton magnetization, indicating that zz -order relaxes predominantly via nitrogen, eq 2.

From measured R_{IHN} and R_{IH} , longitudinal relaxation rates of nitrogen are calculated using eq 2c: $R_{\text{IN}} = 160 \pm 30 \text{ s}^{-1}$ for KatG and $R_{\text{IN}} = 70 \pm 30 \text{ s}^{-1}$ for KatG(S315T). ^{15}N -Fe distances determined from eq 4 are $r_{\text{Fe-N}} = 3.8 \pm 0.8 \text{ \AA}$ and $r_{\text{Fe-N}} = 4.4 \pm 0.9 \text{ \AA}$ for KatG and KatG(S315T), respectively.

Discussion

In a previous study, distance estimates of INH ring protons to the active site Fe ion of wild-type KatG and KatG(S315T) were reported; within the error of measurement, the ^1H -Fe distances were found to be the same for both enzymes.²

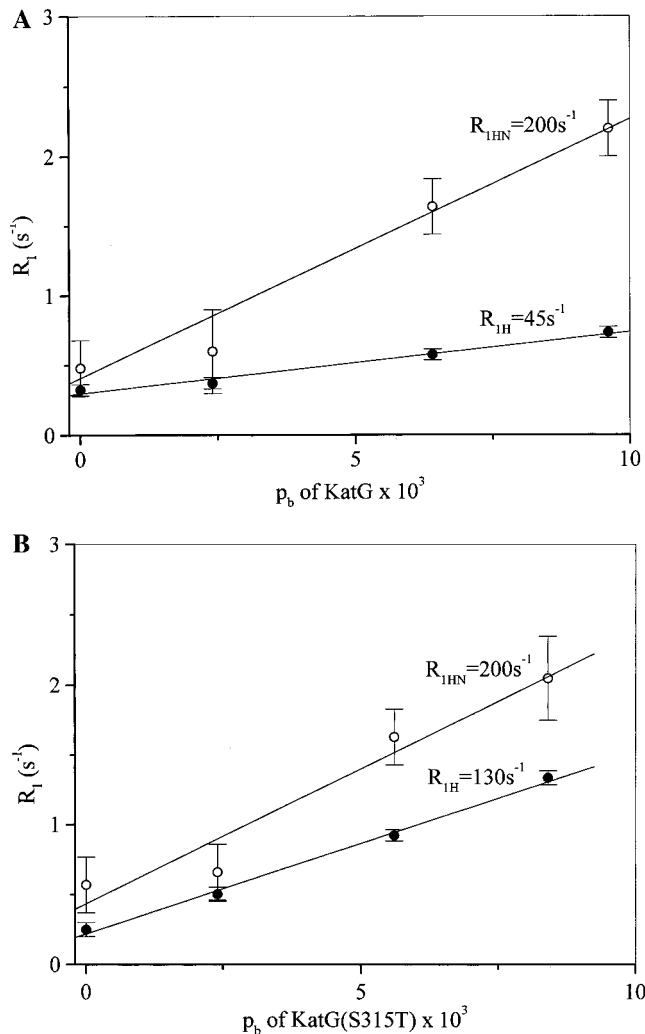


Figure 3. Proton relaxation rate, $R_{\text{IH(obs)}}$ (●), and zz -order relaxation rate (○), $R_{\text{IHN(obs)}}$, as a function of bound protein fraction, p_b , for (A) wild-type KatG and (B) KatG(S315T), obtained by fitting the data to eq 3. Proton relaxation rates, R_{IH} , and relaxation rates of zz -order, R_{IHN} , of the substrate bound to the protein are obtained from the slope of the fit.

Although suggestive of similar isoniazid binding sites for KatG and KatG(S315T), these data were not definitive since the observed relaxation times represented a composite of relaxation times for equivalent protons of the aromatic ring due to the cross-relaxation among the protons of the aromatic system, which tend to eliminate the information on individual proton longitudinal relaxation rates. More generally, if all cross-relaxation paths to a particular spin group are more efficient in transferring magnetization than the differential magnetization leakage, $\sum_i \sigma_{ij} \gg |R_{\text{Ii}} - R_{\text{Ij}}|_{\text{max}}$, all spins relax with a weighted average of individual relaxation rates.³⁴ Cross relaxation in this case, therefore, does not allow the relative orientation of the ligand with respect to Fe center to be determined.

The position of INH to the active site Fe ion might be better constrained using N-Fe distances. However, even with isotopically labeled substrate, it is still necessary to eliminate cross-correlation effects which take place via both dipolar interactions and chemical shift anisotropy.²⁷ As shown in the theoretical section, the simplest way to eliminate cross-correlation effects would be to minimize the primary dipolar interactions, i.e., to design spin-diluted ligand molecules by a suitable isotope

(34) Macura, S.; Ernst, R. R. *Mol. Phys.* **1980**, *41*, 95.

exchange strategy. For protons this can be achieved by fractional deuteration of the substrate molecule. For insensitive nuclei (e.g., ^{13}C , ^{15}N), however, some protons need to be retained for detection; directly bound protons have to be deuterated and indirect detection should rely on heteronuclear coupling to remote protons.

For remotely coupled spin systems, the heteronuclear long-range coupling constant is significantly smaller than the direct coupling constant, and consequently, the time interval required for coupling constant evolution is proportionally longer. In our case, when $^4J_{\text{NH}}$ is ~ 2 Hz (for $^{15}\text{N}_2-^1\text{H}_{3,5}$), a ~ 40 -fold increase of evolution time is required compared to ^{15}N directly bonded to a proton ($^1J_{\text{NH}} \sim 90$ Hz). In paramagnetic systems, where relaxation times are of the order of 10–50 ms, most of the magnetization is lost during this interval, before acquisition. Thus, in paramagnetic systems, the timing of magnetization transfer for indirect detection should be kept as short as possible. Significant gain in signal-to-noise can be achieved, if, instead of detecting the relaxation of z -magnetization of heteronuclei, the relaxation of zz -order can be measured.³⁵ Major improvement comes from the fact that zz -order can be created and detected in half the time needed for longitudinal magnetization detection. The disadvantage of longitudinal zz -order measurements is that the relaxation rate, R_{IHN} , is not necessarily a simple function of the longitudinal relaxation rates of individual spins, R_{IH} and R_{IN} . Consequently, relaxation may not be monoexponential in paramagnetic systems.²⁷ By the use of remote spins, cross-correlation effects are eliminated and zz -order relaxation rate, R_{IHN} , is reduced to a sum of individual longitudinal relaxation rates, R_{IH} and R_{IN} .

Using this approach, the distance between the active site Fe ion and the amide nitrogen of INH was calculated from experimentally determined R_{IN} . From the comparison with previously determined INH proton distances,² we can conclude that the substrate molecule accesses the active site of the enzyme via the hydrazine group. Since the C–N bond of INH undergoes cleavage during enzymatic oxidation to isonicotinic acid, the hydrazine nitrogen must approach the enzyme active site close enough to allow oxidation and/or electron transfer to occur. The obtained ^{15}N –Fe distances fall into a range of distances reported for other heme protein–substrate complexes.^{20–25} They also satisfy the constraints imposed by van der Waals radii of heme

Fe and nitrogen atom and correlate well with the heme iron to guanidino nitrogen distance in nitric oxide synthase complex with L-arginine determined by X-ray³⁶ and ENDOR.³⁷

Interestingly, we find that the distances between the active site Fe ion and the amide nitrogen are, within error, identical for KatG and KatG(S315T). Having in mind the geometry of the INH molecule, Figure 1, these findings do not contradict our earlier reported H–Fe distances,² also being essentially the same for KatG and KatG(S315T). Indeed, they support our previous hypothesis based on EPR, ^1H NMR, and optical data that the differences in the INH binding site of the two enzymes are very subtle and may in fact be insignificant. This should not be surprising since it has been shown that KatG(S315T) retains nearly wild-type levels of catalase and peroxidase activities.^{2,14} Indeed, it suggests that other factors may be responsible for the reduced ability of KatG(S315T) to oxidize INH.^{2,14} One such possibility is that this mutation results in a reduced rate of superoxide binding to the ferric form of KatG(S315T) and, consequently, slower rate of INH oxidation.³⁸ Further higher resolution techniques (e.g. X-ray diffraction) may be required to discern whether there are significant differences in the binding of INH to KatG vs KatG(S315T), enough to explain why this point mutation confers resistance to the drug.

In conclusion, we have proposed a new method of measuring longitudinal relaxation rates of insensitive nuclei (i.e. ^{15}N) in paramagnetic systems via a zz -order created with remote proton. The method is rather straightforward if the nuclei are remote and the cross correlation between them can be neglected. In such cases, zz -order decays monoexponentially. We have demonstrated that the longitudinal relaxation rate of the insensitive nucleus can be obtained simply from the difference between the relaxation rates of zz -order and a remotely coupled proton. By application of this method we have shown that INH penetrates the active center with its hydrazide group close to the heme in both proteins. The obtained ^{15}N binding distances are $r_{\text{Fe-N}} = 3.8 \pm 0.8$ Å from KatG and $r_{\text{Fe-N}} = 4.4 \pm 0.9$ Å from KatG(S315T) Fe ion. The proposed model implies that differences in INH binding site are within the error of our experiment and may not be responsible for INH resistance of KatG(S315T).

Acknowledgment. The authors would like to thank Nikolai R. Skrynnikov for stimulating discussions and Jerry Mohring and Christopher DeGraffenreid for helpful advice regarding the synthesis of isotopically labeled INH. This work was supported by the Mayo Foundation.

JA9918674

(35) Skrynnikov, N. R.; Ernst, R. R. *J. Magn. Reson.* **1999**, *137*, 276.

(36) Henriksen, A.; Schuller, D. J.; Meno, K.; Welinder, K. G.; Smith, A. T.; Gajhede, M. *Biochemistry* **1998**, *37*, 8054.

(37) Tierney, D. L.; Martasek, P.; Doan, P. E.; Masters, B. S. S.; Hoffman, B. M. *J. Am. Chem. Soc.* **1998**, *120*, 2983.

(38) Wengenack, N. L.; Hoard, H. M.; Rusnak, F. M. *J. Am. Chem. Soc.* **1999**, *121*, 9748.